

## Compatible Blends of Polypropylene with an Amorphous Polyamide

N. Aranburu, J. I. Eguiazabal

Departamento de Ciencia y Tecnología de Polímeros and Instituto de Materiales Poliméricos "POLYMAT," Facultad de Ciencias Químicas UPV/EHU, 20080 Donostia, Spain

Correspondence to: J. I. Eguiazabal (E-mail: josei.eguiazabal@ehu.es)

**ABSTRACT:** Compatible polymer blends of polypropylene (PP) with an amorphous polyamide (aPA) were obtained through reactive compatibilization by adding 20% maleic anhydride-modified copolymer (PP-g-MA) to the blends. The blends were made up of a pure PP phase and an aPA-rich phase where very small amounts of PP were detected. The dispersed phase particle size decreased considerably indicating that compatibilization occurred. Young's modulus of the compatibilized blends increased with respect to that of the uncompatibilized ones. The compatibilized blends were highly ductile, and the impact strength also improved, proving that compatibilization occurred under a broad range of experimental conditions. © 2012 Wiley Periodicals, Inc. *J. Appl. Polym. Sci.* 000: 000–000, 2012

**KEYWORDS:** blends; compatibilization; mechanical properties; morphology; structure-property relations

Received 1 June 2011; accepted 21 May 2012; published online

**DOI:** 10.1002/app.38090

### INTRODUCTION

It is commonly accepted that, given the generally immiscible nature of polymer blends,<sup>1</sup> compatibilization is a fundamental question.<sup>2</sup> Many compatibilization techniques have been used in the past and are still currently being used to bring about interfacial adhesion in order to obtain the finely dispersed minor phase necessary to produce the desired mechanical properties.<sup>3</sup> Among the compatibilization techniques used are the chemical modification of one of the blend components,<sup>4–6</sup> the promotion of reactions in the melt state,<sup>7,8</sup> the addition of a third component,<sup>9,10</sup> and even the optimization of processing conditions.<sup>11,12</sup>

It is known that while polypropylene (PP) is a low-cost, easy-to-process polymer that presents good mechanical and moisture barrier properties, its high permeability to oxygen and many organic solvents limits its potential use. On the other hand, polyamides (PA) exhibit excellent mechanical and thermal properties, but have some limitations for end uses, such as poor dimensional stability and poor barrier properties. Therefore, it is clear that PP and PA complement each other's properties.

PP/PAs blends, unfortunately, are immiscible and incompatible through the whole composition range due to their polar/non-polar character, giving rise to unviable materials for practical use. For this reason, reactive compatibilization, for instance, has been widely used in these blends, where compatibilizing agents such as maleic anhydride (MA),<sup>3,6,10,13–31</sup> acrylic acid (AA),<sup>6,24,29,31–34</sup> or glycidyl methacrylate (GMA)<sup>26,35–37</sup> linked

to the PP have been used. These groups are able to react with the terminal amine groups in the PA, producing a graft copolymer which locates at the interface. This improves interfacial compatibility resulting from the interaction of the different segments with their respective components,<sup>17,27</sup> leading to improved dispersion of the minor phase and enhancing the adhesion between the two blend components. As these compatibilizers do not selectively locate at the interfaces, but they are fully miscibilized in the matrix, their amount is usually high, i.e., around 20%.<sup>3,13,30</sup>

Amorphous polyamides (aPAs) are relatively new thermoplastics with irregular chemical structures that hinder crystallization. They present attractive properties such as good dimensional stability, good dielectric and barrier properties, and reduced water sorption when compared with crystalline PA<sup>38</sup> but, at the same time, their melt viscosity is higher. PP, on the other hand, has low melt viscosity and none of the aforementioned limitations of the PA; consequently, it is an ideal candidate for blending with aPA. There are, however, few articles on the compatibilization of PP/aPAs blends. PP-g-MA has been used in PP blends with aPA based on (i) isophthalic acid, 12-aminododecanoic acid, and bis(4-amino-3-methyl cyclohexyl) methane,<sup>30</sup> (ii) 1,3-benzenedicarboxylic acid, 1,4-benzenedicarboxylic acid, 1,6-hexanediamine, and 4,4'-methylenebis[2-methylcyclohexanamine],<sup>28</sup> and also on (iii) 1,3-benzenedicarboxylic acid, 1,4-benzenedicarboxylic acid, and 1,6-hexanediamine.<sup>19</sup> However, to our knowledge no article exists that researches the effects of compatibilization on the mechanical properties of PP/aPAs blends.

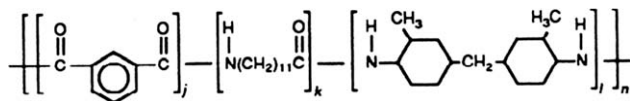


**Figure 1.** Chemical structure of the commercial aPA used in this work.

In this work, a PP-g-MA copolymer was used to analyze its effects on the compatibility of PP-rich blends with an aPA based on isophthalic acid, 12-aminododecanoic acid, and bis(4-amino-3-methylcyclohexyl) methane. The blends were characterized by dynamic-mechanical analysis (DMA) and differential scanning calorimetry (DSC), and their compatibility was tested by means of observing the changes in their morphology and mechanical properties.

## EXPERIMENTAL

The isotactic PP used was ISPLEN PP070 G2M (Repsol YPF, melt flow index (MFI): 12 at 230°C and 2.16 kg load). The aPA was GRILAMID TR55, a random copolymer of isophthalic acid, 12-aminododecanoic acid, and bis(4-amino-3-methylcyclohexyl) methane (EMS Grivory, MFI: 16.0 at 275°C and 5 kg load). Its chemical structure is given in Figure 1. The compatibilizer (PP-g-MA) was FUSABOND PMZ203D, a maleated PP with an average content of 0.74% MA (DuPont, MFI: 102 at 190°C and 2.16 kg load). Drying before processing was performed at 50°C in an air circulation oven for 4 h for PP-g-MA, and at 100°C in a vacuum oven for 24 h in the case of aPA.

Mixing of PP and PP-g-MA to obtain gPP was performed in a Collin ZK25 co-rotating twin screw extruder-kneader. The screw diameter and the  $L/D$  ratio were 25 mm and 30, respectively. A melt temperature of 200°C and a screw rotation rate of 200 rpm were used. The extrudates were cooled in a water bath and pelletized. Then, both the blends of gPP or PP with aPA were obtained separately by direct mixing/injection molding in a Battenfeld BA-230E reciprocating screw injection molding machine to obtain tensile (ASTM D638, type IV, thickness 1.84 mm) and impact (ASTM D256, thickness 3.1 mm) specimens of the pure polymers and the uncompatibilized and compatibilized PP/aPA blends. The screw of the plasticization unit was a standard screw with a diameter of 18 mm,  $L/D$  ratio of 17.8 and a compression ratio of 4. The melt temperature was 265°C and the mold temperature was 15°C. The injection speed and pressure were 10.2 cm<sup>3</sup>/s and 2750 bar, respectively. The specimens were left for 24 h in a dessicator before testing.

Dynamic mechanical analysis of the blends was carried out in a TA Instruments DMA Q800 apparatus at a constant heating rate of 4 °C/min and at a frequency of 1 Hz. The melting behavior of PP was studied by DSC using a Perkin-Elmer DSC-7 calorimeter at 20 °C/min. The melting temperature ( $T_m$ ) and enthalpy ( $\Delta H_m$ ) of PP were determined from the heating scans using the temperature of the maximum and the peak area, respectively. However, these values were not used to analyze the crystallinity of PP in the blends because the melting of PP and the glass transition of aPA ( $T_m = 168$  and  $T_g = 155$ °C, respectively) partially overlapped. The crystallization temperature ( $T_c$ ) and the crystallization enthalpy ( $\Delta H_c$ ) of PP were determined from the cooling

scans using the temperature of the minimum and the peak area, respectively. The crystallinity was calculated assuming a crystallization enthalpy of 137.9 J/g<sup>26</sup> for 100% crystalline PP.

Cryogenically broken surfaces of the tensile specimens of the blends were observed by scanning electron microscopy (SEM) using a Hitachi S-2700 electron microscope that operated at 15 kV.

The melt viscosity of the pure components has been studied by means of torque viscosity in a DSM MICRO 5cc mini-extruder. A melt temperature of 265°C and a screw rotation rate of 50 rpm were used.

The infrared analysis was carried out in a Nicolet 6700 spectrophotometer. The samples were obtained by hot pressing at 180°C with a Collin P 200E press after aPA phase extraction with benzyl alcohol.

Tensile testing was carried out using an Instron 4301 machine at a cross-head speed of 10 mm/min and at (23 ± 2)°C and (50 ± 5)% relative humidity. Young's modulus was determined using an extensometer at a cross-head speed of 1 mm/min. A minimum of five tensile specimens were tested for each reported value. Taking into account the ability of PP and its derivatives to cold draw, ductility was measured as the reduction of area at break. Izod impact tests (ASTM D-256) of unnotched specimens were carried out using a CEAST 6548/000 pendulum on a minimum of eight specimens for each reported value.

## RESULTS AND DISCUSSION

### Optimization of the Compatibilizer Content

A prospective study was carried out to test whether compatibilization occurred, and to choose the optimum compatibilizer (PP-g-MA) content. This study focuses on ductility behavior because it is known that ductility is probably the best polymer blend property<sup>2</sup> to consider when assessing compatibilization.

Figure 2 shows the ductility of the 75/25 blends, measured as the area reduction at break, against the PP-g-MA content. The plot of the elongation at break showed the same characteristics.

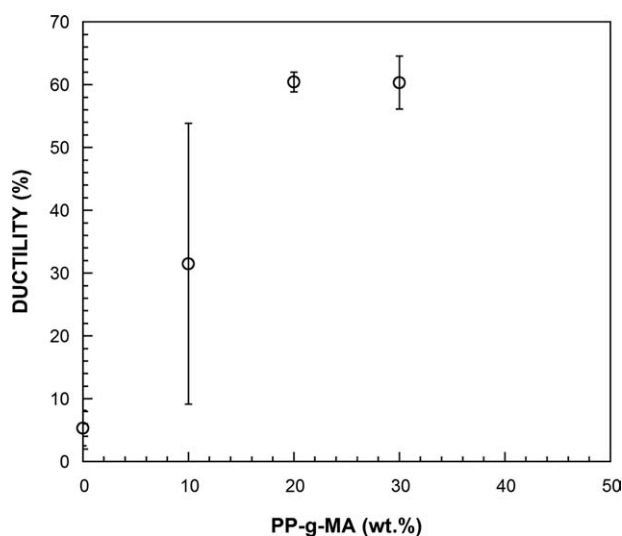


**Figure 2.** Ductility of 75/25 PP/aPA composition blend as a function of PP-g-MA content.

**Table I.** Glass Transition Temperatures of gPP/aPA Blends

Sample	$T_g$ (PP) (°C)	$T_g$ (aPA) (°C)
gPP	6.5 (9.0)	–
gPP/aPA 85/15	5.5 (8.5)	151.5 (154.0)
gPP/aPA 75/25	7.0 (8.5)	151.5 (154.0)
gPP/aPA 60/40	7.0 (9.5)	152.0 (154.0)
gPP/aPA 50/50	6.0 (8.5)	154.0 (155.0)
aPA	–	157.0

The values for the PP/aPA blends are in parentheses. The average standard deviation is 0.5°C.

As can be seen, the ductility of the 0% PP-g-MA blend (vertical axis) was only 5%. This value is very different from that of the pure PP (>80%) and led to a brittle fracture. Some of the blends with 10% PP-g-MA appeared ductile while others did not. However, at 20% PP-g-MA, ductility attained a maximum value (60%) which was roughly 12-fold that of the uncompatibilized blend, and close to that of the pure PP. At higher PP-g-MA contents, ductility persisted. The leveling off or decrease in mechanical properties above a critical compatibilizer content is common in polymer blends.<sup>13,39,40</sup> It is believed that below the optimum level, the interface is not saturated with compatibilizer. Above the optimum level, the compatibilizer saturates the interface,<sup>16</sup> and some compatibilizer stays outside the interface; this is not its function, and may lead to lower homogeneity of the whole blend.<sup>41</sup> Consequently, a 20% PP-g-MA content was selected as the optimum compatibilizer content to be used in the blends for this study.

### Phase Behavior

The phase characteristics of the blends were studied by both DSC and DMA. The melting temperature of PP by DSC (168°C) remained constant in the blends, as expected.<sup>10,21,42</sup> The crystallization temperature of PP during cooling (105°C) increased slightly both in the blends and in the presence of compatibilizer; this indicates a slight nucleating effect of both the aPA and the PP-g-MA. The nucleating effect of PA on the crystallization process of PP has often been reported in literature.<sup>43,44</sup> The crystallinity of PP was unaffected by either the aPA content or the presence of PP-g-MA, and remained steady roughly 65% in the blends with a gPP matrix. It decreased slightly to approximately 50% in the 50/50 composition, which is attributed to the hindered mobility of the PP in the presence of the solid aPA particles during crystallization. This change in the crystalline content is not significant enough to affect the mechanical properties of the blends.

The  $T_g$ s of the blends studied by DMA are summarized in Table I and the representative curves of the 75/25 PP/aPA and gPP/aPA blends, as well as those of the neat aPA and gPP, are shown in Figure 3. It can be observed that gPP shows a single  $T_g$ , as was expected because of the known<sup>25</sup> full miscibility between pure PP and pure PP-g-MA. As can be seen, the low temperature  $T_g$  was always similar to that of the pure PP indicating the presence of an almost pure amorphous PP phase in the blends. The high temperature  $T_g$  decreased marginally at increasing gPP

contents, as can be observed in Figure 3 for the 75/25 gPP/aPA blend. As the decrease is too great to be due to interface interaction induced by the compatibilizer,<sup>45</sup> it is attributed to the presence of some PP, probably of low molecular weight, within the aPA phase. The presence of PP in the aPA-rich phase is, however, minimal (roughly 2.4% when estimated using the Fox equation).

### Phase Morphology

The morphology of the dispersed particles was observed by SEM of the cryofractured surfaces. Figure 4 shows the morphology of the 85/15 and 60/40 blends with a PP matrix both without [Figure 4(a, b)] and with compatibilizer [Figure 4(c, d)]. The 75/25 blends showed intermediate morphologies.

As can be seen in Figure 4, the blends with PP show long (some of them close to 0.5 mm), thick (typically 1.5  $\mu\text{m}$  diameter) and irregularly shaped dispersed particles with a fiber-like morphology. The particle surfaces are smooth and clear. These aspects are clear evidence of poor adhesion and incompatibility, as seen in polyamide-66/polypropylene (PA66/PP)<sup>46</sup> or polypropylene/polyamide-6 (PP/PA6)<sup>47</sup> blends. As can also be seen, some PP particles are occluded within the aPA dispersed domains. If we bear in mind the fundamental incompatibility of the blend, this would suggest that the blending procedure was acceptable.

In the gPP/aPA blends, however, a drastic reduction of the particle size was observed. This indicates the suitability of the used compatibilizer content even in the case of the 40% aPA blend. The fracture surface is rough, and the presence of observable dispersed particles is only limited to small areas of the blends. One of these areas is that shown in Figure 4(d), where very small dispersed particles ( $\sim 0.2 \mu\text{m}$ ) can be seen. Adhesion clearly improved as most aPA particles were visibly integrated in the matrix and debonding was not observed. Roeder et al.<sup>48</sup> also observed a decrease in the diameter of the PA6 phase domains and greater interfacial adhesion between the domains

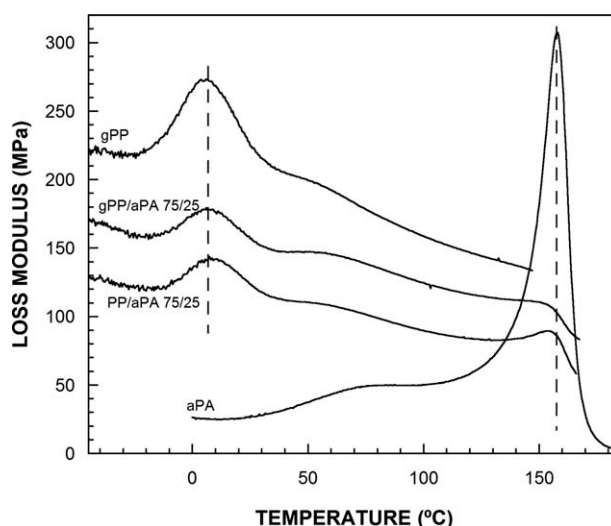


**Figure 3.** Loss modulus curves of the neat aPA, gPP, and the 75/25 PP/aPA and gPP/aPA blends.

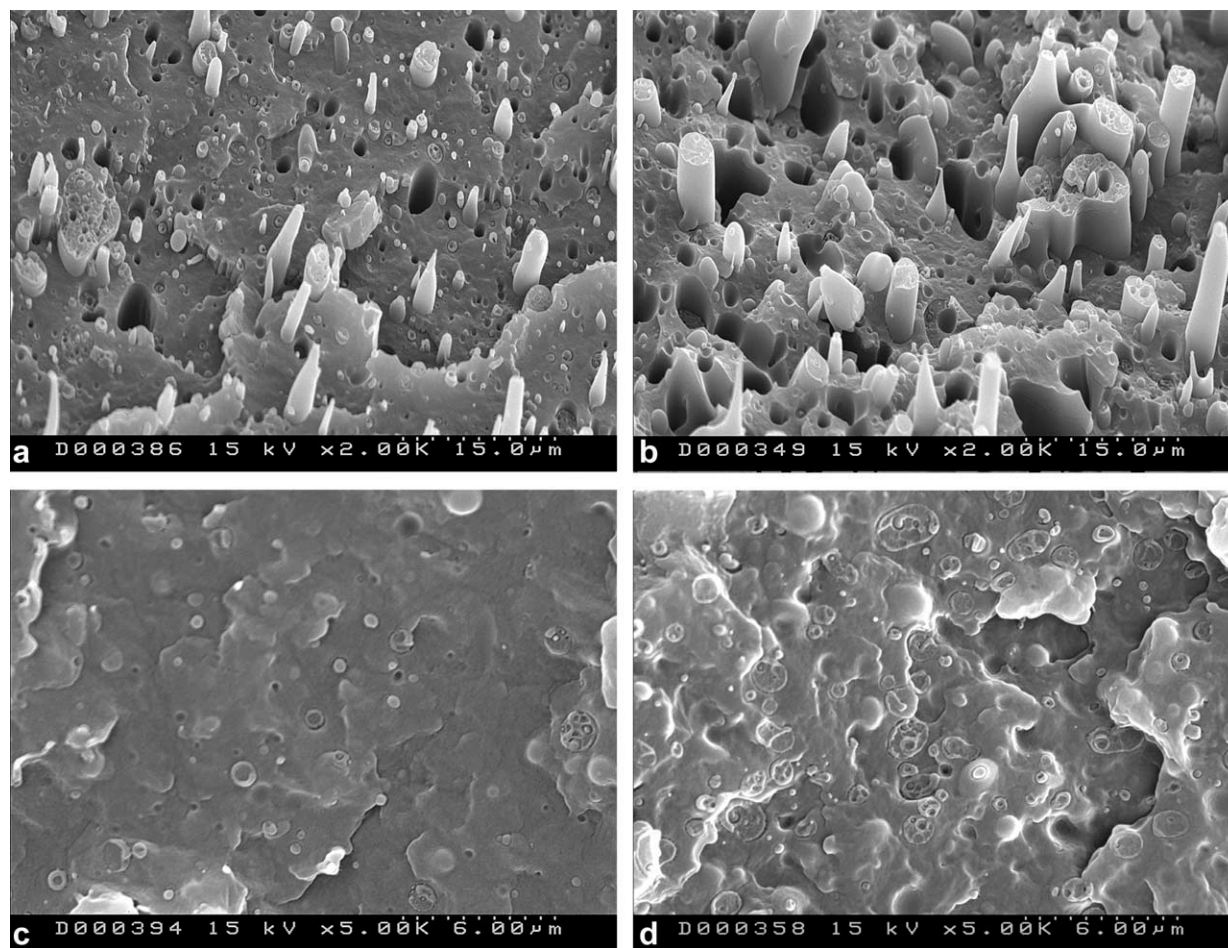


**Figure 4.** SEM micrographs of (a) 85/15 PP/aPA, (b) 60/40 PP/aPA, (c) 85/15 gPP/aPA, and (d) 60/40 gPP/aPA blends.

and matrix upon addition of PP-g-MA compatibilizer to a 70/30 PP/PA6 blend.

It is known that the melt rheology of the blends has a significant effect on the particle size. This is shown with the Taylor equation which defines the relationship between the critical capillary number and the viscosity ratio. Therefore the torque of the two components of the blends was analyzed, as an indirect measurement of viscosity. That of the pure aPA was 3400 N.m and that of the gPP was 450 N.m. As can be seen in the blends of this study, the viscosity of the gPP matrix is much lower than that of the dispersed aPA phase. This, in theory, should lead to a large particle size. However, just the opposite is seen in Figure 4(c, d), which is additional experimental evidence of the considerable compatibilizing effect of the PP-g-MA present in the blends.

The chemical nature of the compatibilized blends was studied by extraction of the aPA phase and FTIR spectroscopy. As seen in Figure 5, although the aPA phase could not be completely extracted from the PP/aPA blends (the  $1640\text{ cm}^{-1}$  band of the amide carbonyl groups was observable in the spectra of the insoluble fraction), the intensity of the peak corresponding to the amide carbonyl groups in the insoluble PP fraction of the gPP/aPA blends is higher. To quantify the remaining aPA con-

tent in the insoluble fraction of the blends, normalization of the  $1640\text{ cm}^{-1}$  peak area was carried out with respect to a PP characteristic band ( $900\text{ cm}^{-1}$ ). As can be observed in Table II, the remaining aPA content for compatibilized 75/25 and 50/50 gPP/aPA blends was roughly 3-fold that of uncompatibilized blends. This indicates the presence of additional reacted aPA, most probably in the form of PP-g-aPA copolymer which is not soluble in benzyl alcohol. The formation of PP-g-PA6 grafted copolymers by *in situ* reaction of the anhydride groups of the

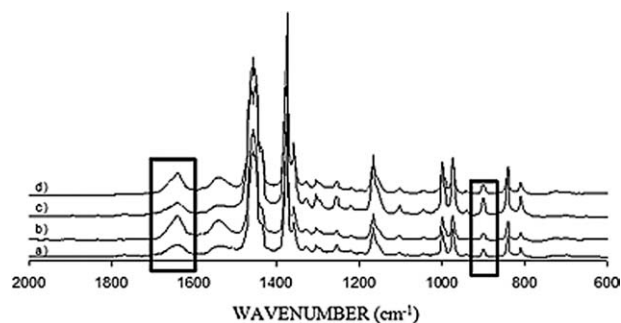


**Figure 5.** FTIR spectra of (a) 75/25 PP/aPA, (b) 75/25 gPP/aPA, (c) 50/50 PP/aPA, and (d) 50/50 gPP/aPA blends.

**Table II.** Remaining aPA Content in 75/25 and 50/50 PP/aPA and gPP/aPA Blends After Partial aPA Extraction

Sample	$A_{aPA}$ (1650 $cm^{-1}$ )	$A_{PP}$ (900 $cm^{-1}$ )	A
PP/aPA 75/25	12.499	1.794	6.967
gPP/aPA 75/25	21.713	1.279	16.976
PP/aPA 50/50	13.980	3.389	4.125
gPP/aPA 50/50	22.094	1.850	11.943

PP-g-MA with the amine end groups of PA6 has been seen in gPP/PA6 blends.<sup>17</sup> These copolymers obviously locate at the interface and consequently decrease interfacial tension<sup>19</sup> and the equilibrium particle size. A smaller particle size leads to an increase in contact area which, in turn, means adhesion is enhanced.

### Mechanical Properties

Young's moduli of both the compatibilized and uncompatibilized blends are plotted in Figure 6 as a function of the aPA content. All the mechanical properties of the gPP/aPA blends are summarized in Table III. The plot of the yield stress was very similar to that of Young's modulus, with a yield stress increase of nearly 30% from the pure PP (29 MPa) to that of the compatibilized 40% aPA blend (39 MPa). As can be observed, the moduli of the compatibilized blends were higher than those of the uncompatibilized blends, and moreover coincided with the linear extrapolation between those of the two pure components. When the cause of the increase in the modulus is examined, the PP crystallinity (phase behavior section) can be ruled out as it was the same in the PP, gPP, and in their blends. We can also rule out the specific volume of the blends because their plot against composition was linear. The orientation was estimated by means of birefringence measurements and the results obtained are shown in Table IV. As can be seen, orientation of the compatibilized blends was higher, which explains the resulting higher modulus. However, the orientation

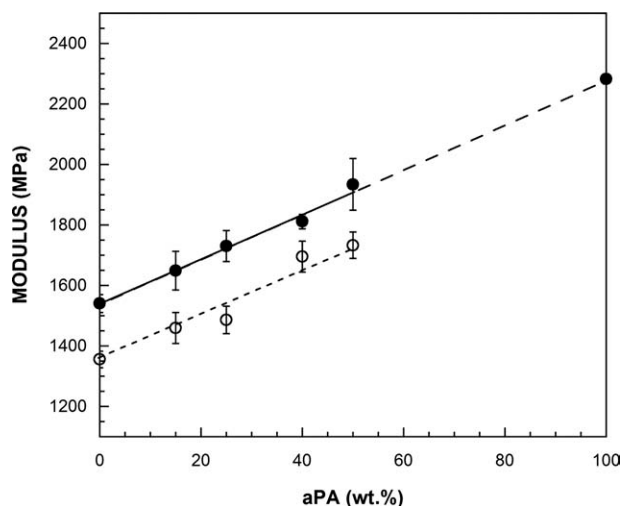


**Figure 6.** Young's modulus of the compatibilized gPP/aPA ([cirf]) and uncompatibilized PP/aPA ([ciro]) blends as a function of the aPA content.

**Table III.** Mechanical Properties of the gPP/aPA Blends as a Function of the Blend Composition

Sample	Young's modulus (MPa) ( $\pm 50$ )	Yield strength (MPa) ( $\pm 0.5$ )	Ductility (%) ( $\pm 4$ )	Unnotched impact strength (J/m) ( $\pm 50$ )
gPP	1550	29	No break	1000
gPP/aPA 85/15	1650	33	70	1000
gPP/aPA 75/25	1750	35	60	1000
gPP/aPA 60/40	1800	39	35	1300
gPP/aPA 50/50	1950	42	5	900
aPA	2300	76	45	No break

The average standard deviations are given inside parentheses.

**Table IV.** Birefringence Values of gPP/aPA Blends

Sample	Birefringence
gPP	$9.4 \times 10^{-3} \pm 1.5 \times 10^{-3}$ ( $4.8 \times 10^{-3} \pm 6.9 \times 10^{-4}$ )
gPP/aPA 85/15	$8.5 \times 10^{-3} \pm 9.5 \times 10^{-4}$ ( $6.8 \times 10^{-3} \pm 7.4 \times 10^{-4}$ )
gPP/aPA 75/25	$8.8 \times 10^{-3} \pm 9.1 \times 10^{-4}$ ( $6.1 \times 10^{-3} \pm 1.0 \times 10^{-3}$ )
gPP/aPA 60/40	$8.8 \times 10^{-3} \pm 1.0 \times 10^{-3}$ ( $6.9 \times 10^{-3} \pm 1.8 \times 10^{-3}$ )
gPP/aPA 50/50	$7.7 \times 10^{-3} \pm 1.3 \times 10^{-3}$ ( $5.8 \times 10^{-3} \pm 2.0 \times 10^{-3}$ )

The values for the PP/aPA blends are in parentheses.

was independent of the aPA content; therefore, it does not influence the modulus of the blends, which depends only on the modulus of the two pure components.

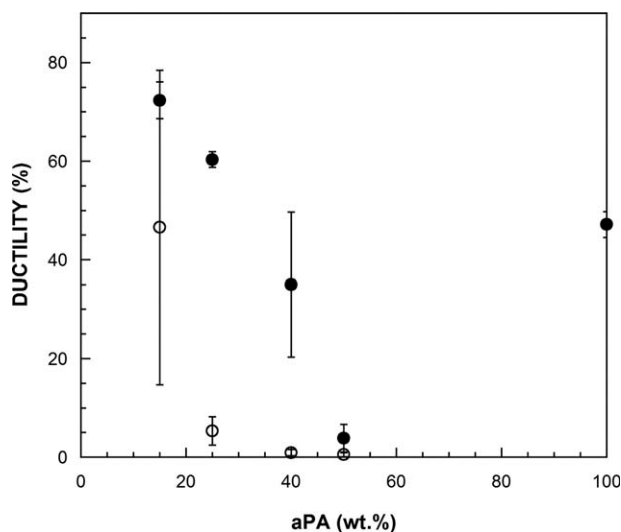


**Figure 7.** Ductility of the compatibilized gPP/aPA ([cirf]) and uncompatibilized PP/aPA ([ciro]) blends as a function of the aPA content.

**Table V.** Unnotched Impact Strength of gPP/aPA Blends

Sample	Unnotched impact strength (J/m)
gPP	976 ± 46 (894 ± 23)
gPP/aPA 85/15	1024 ± 146 (434 ± 36)
gPP/aPA 75/25	979 ± 49 (338 ± 45)
gPP/aPA 60/40	1309 ± 52 (293 ± 21)
gPP/aPA 50/50	890 ± 64 (277 ± 40)
aPA	No break

The values for the PP/aPA blends are in parentheses.

The ductility of the blends is shown in Figure 7. The plot of the elongation at break was similar for all the blends, but showed greater decreases because the ability to cold draw is highly sensitive to changes in ductility. The ductility value (the specimens did not break in the tensile test) (not shown in Figure 7) for both gPP and PP was 80% area reduction (elongation at break: 400%). The compatibilized blends were ductile, i.e., they fully yielded, and in addition, as can be seen in Figure 7, the increase in ductility upon compatibilization was spectacular. This is the best evidence of compatibilization. The ductile nature of the blends together with significant interfacial adhesion<sup>10</sup> is the result of the compatibilizing activity of PP-g-aPA copolymers.<sup>18</sup>

The effect of the addition of two PP-g-MA, containing different MA contents, on the ductility of PP/PA66 75/25 blends has been analyzed.<sup>27</sup> The best results were observed with 20% PP-g-MA containing low-anhydride content and with 2.5% PP-g-MA containing high-anhydride content. The highest elongation at break values were 56% and 19%, respectively. The authors attributed these improvements to the reduction in particle size and improved adhesion resulting from the formation of the graft copolymers. This effect is similar to that seen in this paper and serves as further proof of the significant compatibilizing process of the blends in this study.

It is known that both PP and aPA are very notch-sensitive and low-impact strength materials. In order to find out whether the biphasic nature of the blends is a factor which has a negative effect on toughness, the unnotched impact strength of the blends is shown in Table V as a function of the aPA content. As can be seen, the fragilization typical of multicomponent materials does not occur in these compatibilized gPP-rich blends, because the impact strength of the blends containing gPP (unlike those containing PP) is very similar to that of the single matrix. Moreover, the impact strength of the blends with gPP is clearly greater (3- to 4-fold) than that of the blends with PP. This shows, on the one hand, that the level of adhesion was good enough for the impact tests, which are not usually very demanding in this regard and, on the other, it shows that compatibilization also affected the result of the impact tests, where the stress conditions are much more complex and the test speed at least one magnitude order larger.

## CONCLUSIONS

Compatible PP/aPA blends rich in PP were obtained by melt processing, using 20% PP-g-MA as the compatibilizer. The com-

patibilized blends were made up of two almost pure amorphous gPP and aPA phases. Very low PP contents (roughly 2.4%), most likely of low molecular weight, are present in the aPA phase. The crystallinity of both the gPP and the PP was unaffected by the aPA content.

The addition of the compatibilizer to the blends led to both a significant decrease in the dispersed phase particle size (roughly from 1–2 to 0.2  $\mu\text{m}$ ) and an improvement in interfacial adhesion. This was attributed to the formation of PP-g-aPA grafted copolymers by an *in situ* reaction of the anhydride groups of the PP-g-MA with the amine end groups of aPA as well as to their location at the interface.

The modulus of the blends increased upon compatibilization, but the most relevant result was the spectacular improvement in ductility which yielded blends with unusually positive values for both area reduction and elongation at break. Compatibilization also extended to impact strength since it also occurred at fast test speeds and complex stress conditions.

## ACKNOWLEDGMENTS

The financial support of the Basque Government (project number GIC07/48-IT-234-07) and of the University of the Basque Country (UFI11/56) is gratefully acknowledged. N. Aranburu also acknowledges the Basque Government for the award of a grant for the development of this work.

## REFERENCES

- Datta, S.; Lohse, D. J. *Polymeric Compatibilizers: Uses and Benefits in Polymer Blends*; Hanser Publishers: Munich, 1996.
- Paul, D. R.; Bucknall, C. B. *Polymer Blends*; Wiley-Interscience: New York, 2000.
- Manning, S. C.; Moore, R. B. *Polym. Eng. Sci.* **1999**, *39*, 1921.
- Koulouri, E. G.; Georgaki, A. X.; Kallitsis, J. K. *Polymer* **1997**, *38*, 4185.
- Kim, B. K.; Park, S. Y.; Park, S. J. *Eur. Polym. J.* **1991**, *27*, 349.
- Nagel, J.; Scheidler, D.; Hupfer, B.; Bräuer, M.; Pleul, D.; Vogel, C.; Lehmann, D.; Amesöder, S. *J. Appl. Polym. Sci.* **2006**, *100*, 2992.
- Ou, C.-F.; Lin, C.-C. *J. Appl. Polym. Sci.* **1996**, *59*, 1379.
- Wei, K.-H.; Ho, J.-C. *Macromolecules* **1997**, *30*, 1587.
- Wei, Q.; Chionna, D.; Pracella, M. *Macromol. Chem. Phys.* **2005**, *206*, 777.
- Holsti-Miettinen, R.; Seppälä, J. *Polym. Eng. Sci.* **1992**, *32*, 868.
- Eguiazabal, J. I.; Nazabal, J. *Plast. Rubber Process. Appl.* **1990**, *14*, 211.
- Narh, K. A.; Zhang, Q.; Li, Z. *J. Appl. Polym. Sci.* **2000**, *75*, 1783.
- Cartier, H.; Hu, G.-H. *Polym. Eng. Sci.* **1999**, *39*, 996.
- Abacha, N.; Fellahi, S. *Polym. Int.* **2005**, *54*, 909.
- Jose, S.; Francis, B.; Thomas, S.; Karger-Kocsis, J. *Polymer* **2006**, *47*, 3874.

16. Jose, S.; Nair, S. V.; Thomas, S.; Karger-Kocsis, J. *J. Appl. Polym. Sci.* **2006**, *99*, 2640.
17. Ide, F.; Hasegawa, A. *J. Appl. Polym. Sci.* **1974**, *18*, 963.
18. Sathe, S. N.; Devi, S.; Rao, G. S. S.; Rao, K. V. *J. Appl. Polym. Sci.* **1996**, *61*, 97.
19. Zhang, J.; Cole, P. J.; Nagpal, U.; Macosko, C. W.; Lodge, T. P. *J. Adhes.* **2006**, *82*, 887.
20. Lu, B.; Chung, T. C. *Macromolecules* **1999**, *32*, 2525.
21. Jaziri, M.; Barhoumi, N.; Massardier, V.; Mélis, F. *J. Appl. Polym. Sci.* **2008**, *107*, 3451.
22. González-Montiel, A.; Keskkula, H.; Paul, D. R. *J. Polym. Sci. Part B: Polym. Phys.* **1995**, *33*, 1751.
23. Li, D.; Jia, D.; Zhou, P. *J. Appl. Polym. Sci.* **2004**, *93*, 420.
24. Jung, C.-H.; Choi, J.-H.; Lim, Y.-M.; Jeun, J.-P.; An, S.-J.; Kang, P.-H.; Nho, Y.-C. *Macromol. Symp.* **2007**, *249–250*, 573.
25. Jose, S.; Thomas, S.; Biju, P. K.; Koshy, P.; Karger-Kocsis, J. *Polym. Degrad. Stab.* **2008**, *93*, 1176.
26. Tedesco, A.; Barbosa, R. V.; Nachtigall, S. M. B.; Mauler, R. S. *Polym. Test.* **2002**, *21*, 11.
27. Duvall, J.; Sellitti, C.; Myers, C.; Hiltner, A.; Baer, E. *J. Appl. Polym. Sci.* **1994**, *52*, 195.
28. Cho, K.; Li, F. *Macromolecules* **1998**, *31*, 7495.
29. Agrawal, P.; Oliveira, S. I.; Araújo, E. M.; Melo, T. J. A. *J. Mater. Sci.* **2007**, *42*, 5007.
30. Li, H.; Chiba, T.; Higashida, N.; Yang, Y.; Inoue, T. *Polymer* **1997**, *38*, 3921.
31. Valenza, A.; Acierno, D. *Eur. Polym. J.* **1994**, *30*, 1121.
32. Liang, Z.; Williams, H. L. *J. Appl. Polym. Sci.* **1992**, *44*, 699.
33. Zhang, X.-M.; Yin, J.-H. *Polym. Eng. Sci.* **1997**, *37*, 197.
34. Dagli, S. S.; Xanthos, M.; Biesenberger, J. A. *Polym. Eng. Sci.* **1994**, *34*, 1720.
35. Zhang, X.; Li, X. L.; Wang, D.; Yin, Z.; Yin, J. *J. Appl. Polym. Sci.* **1997**, *64*, 1489.
36. Zhang, X.; Yin, Z.; Yin, J. *J. Appl. Polym. Sci.* **1996**, *62*, 893.
37. Tedesco, A.; Krey, P. F.; Barbosa, R. V.; Mauler, R. S. *Polym. Int.* **2001**, *51*, 105.
38. García, M.; Eguiazábal, J. I.; Nazabal, J. *Polym. Compos.* **2003**, *24*, 555.
39. Komalan, C.; George, K. E.; Jacob, S.; Thomas, S. *Polym. Adv. Technol.* **2008**, *19*, 351.
40. Chen, G.; Liu, J. *J. Mater. Sci.* **1999**, *34*, 4375.
41. Tang, T.; Huang, B. *Polymer* **1994**, *35*, 281.
42. Torres, N.; Robin, J. J.; Boutevin, B. *J. Appl. Polym. Sci.* **2001**, *81*, 2377.
43. Tseng, F.-P.; Lin, J.-J.; Tseng, C.-R.; Chang, F.-C. *Polymer* **2001**, *42*, 713.
44. Wu, Y.; Yang, Y.; Li, B.; Han, Y. *J. Appl. Polym. Sci.* **2006**, *100*, 3187.
45. Chiu, H.-T.; Hsiao, Y.-K. *J. Polym. Res.* **2006**, *13*, 153.
46. Duvall, J.; Sellitti, C.; Topolkaraev, V.; Hiltner, A.; Baer, E.; Myers, C. *Polymer* **1994**, *35*, 3948.
47. Park, S. J.; Kim, B. K.; Jeong, H. M. *Eur. Polym. J.* **1990**, *26*, 131.
48. Roeder, J.; Oliveira, R. V. B.; Gonçalves, M. C.; Soldi, V.; Pires, A. T. N. *Polym. Test.* **2002**, *21*, 815.